Heliyon 7 (2021) e07182

Contents lists available at ScienceDirect

Heliyon

journal homepage: www.cell.com/heliyon

Research article

# The kinetics of thin-layer drying and modelling for mango slices and the influence of differing hot-air drying methods on quality

Khuthadzo Mugodo *, Tilahun S. Workneh

*Bioresource Engineering, School of Engineering, University of Kwazulu-Natal, Pietermaritzburg, South Africa*

ARTICLE INFO

*Keywords:*
Drying rate
Mango
Modelling
Solar drying
Quality
Thickness

ABSTRACT

This study compared the thin-layer drying kinetics of hot-air methods, namely, convective oven drying (OVD), uncontrolled solar drying (UAD) and modified ventilation greenhouse solar drying (MVD). Additionally, the effects of these drying techniques on colour, rehydration characteristics and microstructure of Tommy Atkin mango slices were investigated. The experiments were conducted on mango slices of three different thicknesses: 3 mm, 6 mm and 9 mm. The drying curves generated from the experimental data revealed that the rate of drying increased with thickness and that a thickness of 3 mm is optimal. It was discovered that increased drying rates resulted in a decrease in the drying time. When 3 mm slices were dried using OVD and MVD, the duration of the drying process was reduced by 85% and 80%, respectively, in comparison to the samples dried under UAD conditions. Lemon juice pre-drying treatment had no significant ($p < 0.05$) effect on the drying rate or duration of the drying process. Non-linear regression analysis was used to optimise the drying coefficients by fitting the moisture ratio data to eleven suitable thin-layer models. The model parameters developed by Midilli et al. performed the best in terms of predicting the experimental moisture ratio ($R^2 = 0.9810$-$0.9981$, $\chi^2 = 1.465 \times 10^{-6}$-$3.081 \times 10^{-5}$ and RMSE = 0.0003-0.0004). Additionally, increasing the slice thickness to 6 mm and 9 mm prolonged the drying times, resulting in significant changes in sample quality, including the total colour (ΔE), rehydration and microstructure. In comparison to OVD- and MVD-dried samples, UAD-dried samples exhibited the greatest colour change and had the highest rehydration ratio values. Also, the surface of the UAD-dried samples developed a more porous structure with distinct cracks. Based on the results, MVD was determined to be a viable alternative method for drying 3 mm mango slices on a large scale.

## 1. Introduction

Mango (*Mangifera indica L.*) is a tropical fruit that is cultivated in over a hundred countries worldwide (Mitra, 2016; Liu et al., 2020). The mango is a fruit widely distributed throughout Asia, Africa and the Central and South America continents. As a result, these three regions produced approximately 74%, 12.8% and 13% of global mango production volume (approximately 55 million during the 2018/19 base period), respectively (FAOSTAT, 2019). Mangoes are grown in the most tropical and subtropical areas of South Africa, which are located in the country's north-eastern region, and the 2018/19 season produced 93870 tons (DAFF, 2018; Tshitiza et al., 2020). Volume production increased by 16% over the 2017/18 season. Notably, global mango consumption per capita has been increasing. According to the FAO's forecast, which was published in Liu et al. (2020), per-capita consumption would increase to approximately 8.3 kg/person/year by 2028. This results from rising incomes in developing countries, including South Africa and corresponding changes in dietary preferences. Tommy Atkin is the most preferred cultivar among retailers and consumers, owing to its attractive colour and relatively long shelf life (Galán Saúco, 2010). The mango fruit's increasing popularity is due to high vitamin A and C content, beta-carotene, high fibre and low calorie content (approximately 110 calories per average size of mango) (DAFF, 2018).

Dried mango occupies a relative niche position in the market, due to its income-generation potential. As one of the highest revenue generators, it has the potential to contribute to food security for smallholder farmers and surrounding communities (Aphane, 2015). Additionally, the majority of fresh mangoes produced by smallholder farmers in Sub-Saharan African countries either spoil in roadside stands or rot where they fall from trees during the peak season, due to market saturation (Mercer, 2012). Consumer preference for healthier snack alternatives, including dried mango is increasing in this region, providing a

* Corresponding author.
*E-mail address:* mugodok@ukzn.ac.za (K. Mugodo).

https://doi.org/10.1016/j.heliyon.2021.e07182
Received 11 February 2020; Received in revised form 22 July 2020; Accepted 27 May 2021

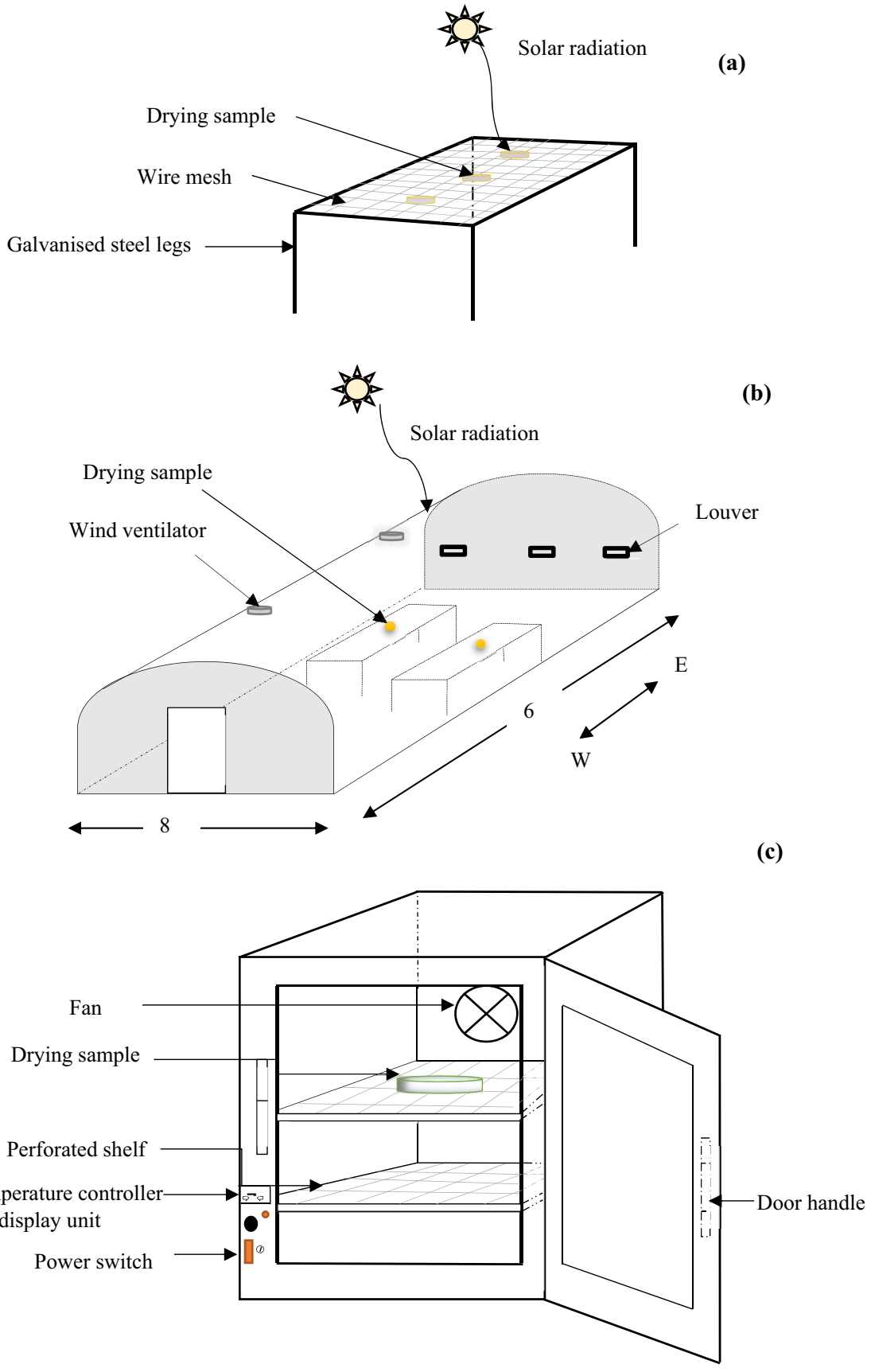


**Figure 1.** Schematic diagrams of (a) uncontrolled solar dryer, (b) modified ventilation greenhouse solar dryer and **(c)** laboratory-scale convective oven dryer (not drawn to scale).

**Table 1.** Drying conditions observed inUAD and MVD.

| Drying method | Day number | Temperature (°C) | Relative humidity (%) | Solar radiation (W.M$^{-2}$) |
|---|---|---|---|---|
| UAD | 1 | 15.55–26.25 | 42.33–79.06 | 438.41–1016.20 |
| | 2 | 23.54–33.43 | 34.83–52.26 | 428.53–992.39 |
| | 3 | 26.22–36.77 | 22.96–58.01 | 317.79–975.63 |
| MVD | 1 | 31.28–56.18 | 10.36–37.39 | 438.41–1016.20 |
| | 2 | 41.00–64.26 | 12.67–24.49 | 428.53–992.39 |

**Table 2.** The applied mathematical models for thin-layer drying.

| Model name | Model equation | References |
|---|---|---|
| Aghabashlo model | $MR = \exp\left(-\frac{k_1}{1+k_2}\right)$ | Aghbashlo et al. (2008) |
| Demir *et al.* | $MR = aexp(-kt^n) + b$ | Demir et al. (2007) |
| Diffusion approximation | $MR = aexp(-kt) + (1-a)(-kbt)$ | Dhanushkodi et al. (2017)<br>Demir et al. (2007) |
| Henderson and Pabis | $MR = aexp(-kt)$ | Motevalli et al. (2013) |
| Hii *et al.* | $MR = aexp(-kt^n) + cexp(-gt^n)$ | Hii et al. (2009) |
| Page | $MR = \exp(-kt^n)$ | Wang et al. (2007) |
| Two term | $MR = aexp(-k_0t) + bexp(-k_1t)$ | Dhanushkodi et al. (2017) |
| Lewis | $MR = \exp(-kt)$ | Deshmukh et al. (2014) |
| Midilli *et al.* | $MR = aexp(-kt^n) + bt$ | Midilli et al. (2002), Hayaloglu et al. (2007) |
| Modified Henderson and Pabis | $MR = aexp(-kt) + bexp(-gt) + cexp(-ht)$ | Meisami-asl and Rafiee (2009) |
| Verma *et al.* | $MR = aexp(-kt) + (1-a)exp(-gt)$ | Verma et al. (1985) |

MR (dimensionless)is the moisture ratio estimated by the model, t (h) is the drying time, k is the drying constant and *a, b, g, h, n* are model coefficients.

much-needed market access for smallholder farmers looking to expand their profitable agribusiness. Additionally, it can assist in minimising postharvest product losses and increasing sales, particularly during the off-season periods of April to November (DAFF, 2018). Traditionally, thin-layer drying has occurred in an uncontrolled environment, with the product exposed to both ambient air and direct sunlight. To a large extent, it is the preferred method of drying for the majority of rural populations in Sub-Saharan Africa (Touré and Kibangu-Nkembo, 2004; ELkhadraoui et al., 2015; Ntuli et al., 2017). Numerous research studies have established that uncontrolled solar drying has flaws that jeopardise the dried product's quality, including extended drying times, microbial growth and infestation by insects (Fadhel et al., 2014; Misha et al., 2016). Additionally, Kumar et al. (2013), discovered that the process was completed with relatively slow drying rates over an extended period of time.

Touré and Kibangu-Nkembo (2004) assert that the absence of an enclosed chamber during drying has an effect on the rate of drying. Alternatively, agricultural commodities have been dried efficiently using common drying technologies, such as convective hot-air drying. Nevertheless, in a country like South Africa, where electricity tariffs are relatively high and load shedding is common, it may be prohibitively expensive to use electricity to remove water in foods (Kumar et al., 2013). Additionally, research into greenhouse/tunnel solar drying technologies has revealed that they offer superior benefits over uncontrolled solar drying, including increased drying rates (Fadhel et al., 2014; ELkhadraoui et al., 2015). An enhanced solar dryer can reduce the drying time by 65% compared to an uncontrolled solar dryer because it generates a higher temperature and lower relative humidity (Basunia and Abe, 2001).

Mercer (2012) compared uncontrolled solar drying and an enhanced direct solar dryer prototype. The improved solar dryer decreased the time required to dry mango slices from 24 to 16 h, compared to uncontrolled solar drying. A greenhouse and indirect natural convection solar dryer reduced the time for red pepper drying by six and forty-five hours, respectively when compared to uncontrolled solar drying. Additionally, Fadhel et al. (2014) asserted the profitability of the natural convective solar dryer. However, it is limited to small-scale drying (El khadraoui et al., 2019). The study concluded that a new hybrid greenhouse solar dryer could reduce the drying time of pepper by seven hours when compared to uncontrolled solar drying under the same climatic conditions. As a result, improved ventilation could enhance the viability of a greenhouse-style solar dryer. The drying kinetics of greenhouse and uncontrolled solar dryers were compared under various climatic conditions; however, in particular for mango fruit, the impact of slice thickness of and pre-drying treatments on product quality was overlooked.

Numerous studies have examined the drying behaviour of a variety of agricultural commodities using model-based analysis (Akoy, 2014a; Deng et al., 2017; Nyangena et al., 2019). This study compared and evaluated how the drying kinetics influences the characteristics of Tommy Atkin mangoes using thin-layer drying models. This was done to compare MVD to OVD and UAD in KwaZulu-Natal, South African climate. In conjuction with the results of the pre-drying treatment and the slicing thickness, both the drying procedure and quality properties of mango slices were assessed.

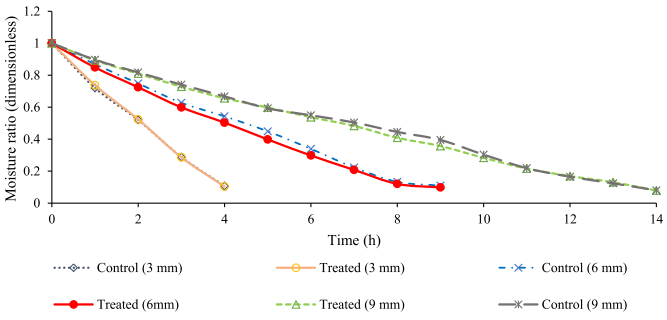


**Figure 2.** Changes in the dimensionless moisture ratio of mango samples during the drying period (MVD).

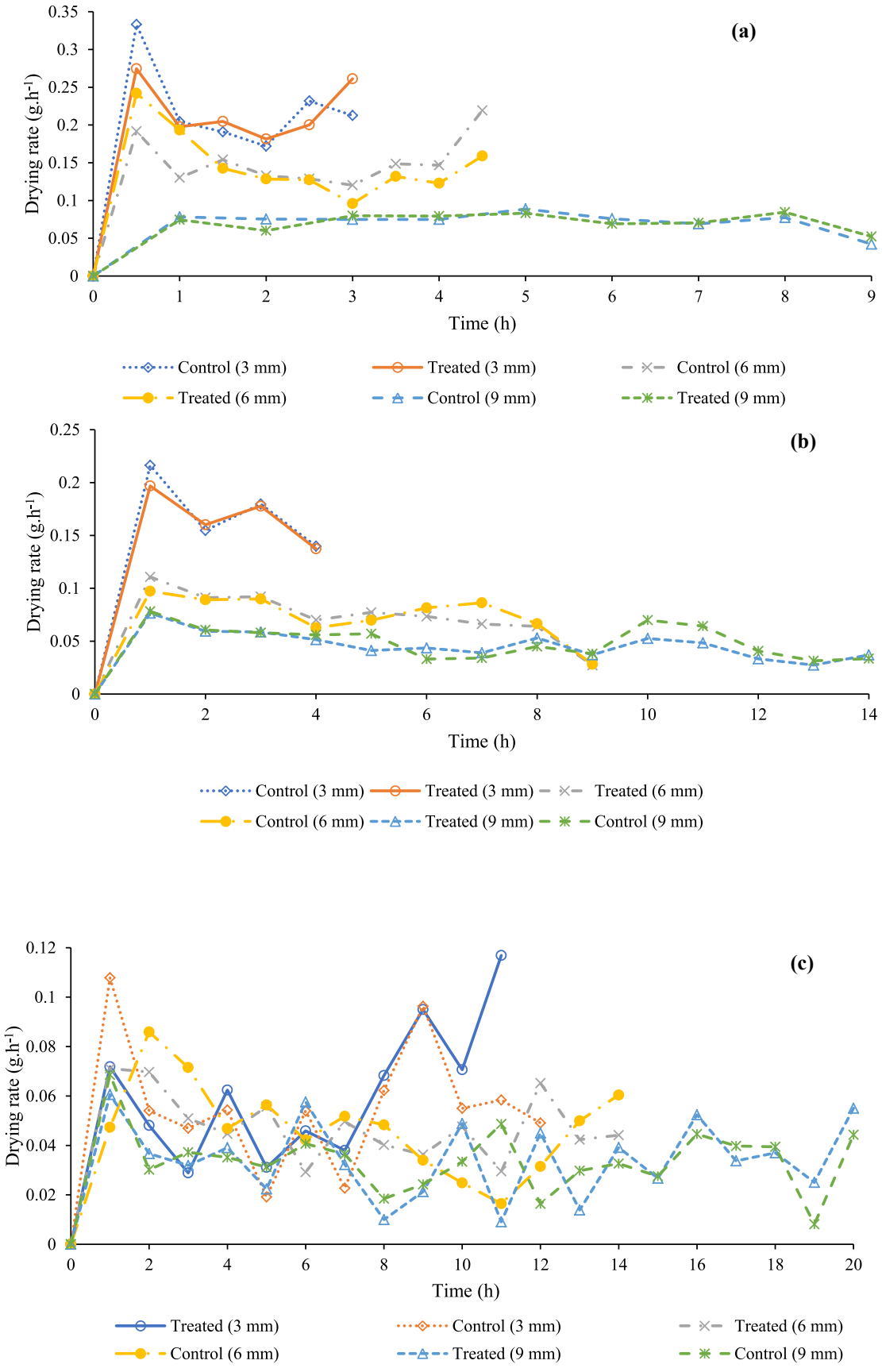


**Figure 3.** The dying rate curves for mango samples dried in (a) OVD, (b) MVD, and (c) UAD.

**Table 3.** Changes in the drying time of the selected drying treatments.

| Drying method | Slice thickness (mm) | Pre-drying treatment | Drying time (h) | % reduction in drying time |
|---|---|---|---|---|
| UAD | 9 | Lemon juice | 20 | 0 |
| | 9 | Control | 20 | 0 |
| | 6 | Lemon juice | 14 | 30 |
| | 6 | Control | 14 | 30 |
| | 3 | Lemon juice | 11 | 45 |
| | 3 | Control | 12 | 40 |
| MVD | 9 | Lemon juice | 14 | 30 |
| | 3 | Control | 14 | 30 |
| | 6 | Lemon juice | 9 | 55 |
| | 6 | Control | 9 | 55 |
| | 3 | Lemon juice | 4 | 80 |
| | 3 | Control | 4 | 80 |
| OVD | 9 | Lemon juice | 8 | 60 |
| | 9 | Control | 8 | 60 |
| | 6 | Lemon juice | 4.5 | 77.5 |
| | 6 | Control | 5 | 75 |
| | 3 | Lemon juice | 3 | 85 |
| | 3 | Control | 3 | 85 |

## 2. Materials and methods

### 2.1. Plant material and pre-drying treatments

Mangoes (Tommy Atkin cultivar) were prepared at a room temperature of about 21.83 °C immediately after delivery at the Food Science laboratory of the University of Kwazulu-Natal, Pietermaritzburg. The mangoes were washed by tap water and the skin was peeled with a hand peeler. They had an average firmness of 4.4 N and 13.85 °Brix total soluble solids (TSS). The fruit was cut into 3 mm, 6 mm, 9 mm slices with a knife, removing the seed. The mango samples were dipped in bottled lemon juice (100 percent) for five minutes. After drying, the samples were placed in plastic bags.

### 2.2. Drying methods experimental set-up

The treated and control mango samples were subjected to (OVD), (UAD) and (MVD), as described in (Mugodo, 2017). In UAD, mango slices were placed on top of a 6 $m^2$ perforated wire mesh that was 1 m above the ground level, as shown in Figure 1a. The UAD and MVD experiments were conducted concurrently from 18 to 20 January 2017 at the Ukulinga Research Farm at Pietermaritzburg, South Africa (29.663° S and 30.405° E, an altitude of 721 m above sea level). MVD was a modified greenhouse structure (48 $m^2$ floor area), constructed of galvanised steel frame and 200 μm polyethylene plastic covering. As illustrated in Figure 1b, the greenhouse was modified to include an air inlet that aided in the natural ventilation system (0.5 × 0.5 m). The minimum and maximum ambient air temperatures and those recorded inside the MVD are listed in Table 1. Figure 1c depicts OVD experiments performed at 70 °C, using a laboratory-scale forced air convective dryer. The dryer was left idle for two hours before placing the samples inside, allowing the dryer to stabilise at the desired temperature. The drying experiments were conducted from a moisture content of 79.2 ± 2% to 10 ± 0.9% on a wet basis. The instantaneous moisture content of mango slices was determined by weighing them at 30 min intervals for OVD and one-hour intervals for the other drying methods. The weight loss was measured by a digital scale with a resolution of 0.1g. The moisture content of fresh mango samples was determined using the AOAC 930.15 method, in which the sample was dried for 2 h at 135 °C (AOAC, 2005). The dimensionless moisture content and drying rate were determined by Eqs. (1) and (3), respectively (Diamante and Munro, 1993).

$$MR = \frac{M_{cx} - M_e}{M_i - M_e} \quad (1)$$

Since the equilibrium moisture content values are relatively low in comparison to the initial ($M_i$) and instantaneous ($M_{cx}$) contents, Eq. (1) was simplified as described in (Diamante and Munro, 1993) and (Workneh and Oke, 2012) to form Eq. (2). The drying rate was calculated by Eq. (3).

$$MR = \frac{M_{cx}}{M_i} \quad (2)$$

$$DR = \frac{M_{t+dt} - M_t}{dt} \quad (3)$$

### 2.3. Mathematical modelling of drying data

The experimental moisture data obtained during drying was converted to the dimensionless moisture content/moisture ratio using Eq. (2). To determine the goodness of fit of eleven existing mathematical models (moisture ratio based), as shown in Table 2, non-linear regression was completed using the SPSS (Statistical Package for Social Science) ver.26 software package. The statistical parameters, coefficient of determination ($R^2$), root mean square error (RMSE) and chi-square ($\chi^2$) were estimated to evaluate the goodness of the models. This was done by the graphical method ($R^2$) and Eqs. (4) and (5) were used to determine the RMSE and $\chi^2$. The model with the highest $R^2$ and the lowest $\chi^2$ and RMSE values exhibited the highest goodness of fit (Goyal et al., 2008).

$$\mathrm{RMSE} = \left( \frac{\sum_{i=1}^{N} \left( \mathrm{MR}_{\mathrm{pre,i}} - \mathrm{MR}_{\mathrm{exp,i}} \right)^2}{N} \right)^{\frac{1}{2}} \quad (4)$$

$$\chi^2 = \frac{\sum_{i=1}^{N} \left( \mathrm{MR}_{\mathrm{pre,i}} - \mathrm{MR}_{\mathrm{exp,i}} \right)^2}{N - z} \quad (5)$$

### 2.4. Estimation of the effective moisture diffusivity

Since the drying process occurred primarily at a falling rate, the Fick's diffusion equation for products with a slab geometry was used in this study to calculate the solution of the effective moisture diffusivity ($D_{eff}$), as shown in Eqs. (6) and (7) (Crank, 1975). Firstly, estimated by plotting

**Table 4.** Goodness of fit parameters obtained by fitting selected moisture ratio models on the experimental data for control samples.

| Model name | Thickness (mm) | Model parameters | | | | | | | | | $\chi^2$ | $R^2$ | RMSE |
|---|---|---|---|---|---|---|---|---|---|---|---|---|---|
| | | k or $k_0$ | $k_1$ | $k_2$ | n | a | b | c | g | h | | | |
| Demil et al.- OVD | 3 | 0.4071 | - | - | 1.3348 | 0.9735 | 0 | - | - | - | $9.8369 \times 10^{-5}$ | 0.9814 | 0.0065 |
| | 6 | 0.2871 | - | - | 1.2049 | 0.9762 | 0 | - | - | - | $9.3303 \times 10^{-5}$ | 0.9885 | 0.0063 |
| | 9 | 0.9718 | - | - | 1.6028 | 0.9717 | 0 | - | - | - | $4.6902 \times 10^{-5}$ | 0.9962 | 0.0045 |
| Demil et al.- UAD | 3 | 0.0257 | - | - | 1.6958 | 0.9093 | 0 | - | - | - | 0.00028 | 0.9665 | 0.0110 |
| | 6 | 0.0894 | - | - | 1.1249 | 1.0039 | 0 | - | - | - | $4.849 \times 10^{-6}$ | 0.9957 | 0.0014 |
| | 9 | 0.0167 | - | - | 1.5807 | 0.9278 | 0 | - | - | - | 0.00051 | 0.9852 | 0.0148 |
| Demil et al. -MVD | 3 | 0.2664 | - | - | 1.4288 | 0.9884 | 0 | - | - | - | $4.256 \times 10^{-5}$ | 0.9913 | 0.0043 |
| | 6 | 0.0818 | - | - | 1.4657 | 0.9705 | 0 | - | - | - | $9.873 \times 10^{-5}$ | 0.9916 | 0.0065 |
| | 9 | 0.0395 | - | - | 1.4844 | 0.9466 | 0 | - | - | - | 0.00039 | 0.9842 | 0.0129 |
| Midilli et al.- OVD | 3 | 0.4071 | - | - | 1.3348 | 0.9735 | 0 | - | - | - | $9.8458 \times 10^{-5}$ | 0.9814 | 0.00649 |
| | 6 | 0.1782 | - | - | 1.5255 | 0.9570 | 0 | - | - | - | 0.02177 | 0.9790 | 0.11431 |
| | 9 | 0.0526 | - | - | 1.6314 | 1.6314 | 0 | - | - | - | $2.6825 \times 10^{-5}$ | 0.9953 | 0.00386 |
| Midilli et al. – UAD | 3 | 0.0257 | - | - | 1.6962 | 0.9092 | 0 | - | - | - | 0.000106 | 0.9665 | 0.00839 |
| | 6 | 0.0894 | - | - | 1.1251 | 1.0039 | 0 | - | - | - | $1.4651 \times 10^{-6}$ | 0.9981 | 0.00102 |
| | 9 | 0.9277 | - | - | 1.5806 | 0.9277 | 0 | - | - | - | $9.5974 \times 10^{-5}$ | 0.9852 | 0.00876 |
| Midilli et al. -MVD | 3 | 0.2663 | - | - | 1.4287 | 0.9883 | 0 | - | - | - | $4.005 \times 10^{-5}$ | 0.9913 | 0.00563 |
| | 6 | 0.0817 | - | - | 1.4662 | 0.9704 | 0 | - | - | - | $5.9059 \times 10^{-5}$ | 0.9916 | 0.00573 |
| | 9 | 0.0395 | - | - | 1.4843 | 0.9466 | 0 | - | - | - | 0.00012 | 0.9842 | 0.00901 |
| Aghabashlo Model- OVD | 3 | - | 0.5153 | 0 | - | - | - | - | - | - | $1.2229 \times 10^{-6}$ | 0.9705 | 0.0134 |
| | 6 | - | 0.0360 | 0 | - | - | - | - | - | - | $1.3159 \times 10^{-5}$ | 0.9841 | 0.0024 |
| | 9 | - | 0.1715 | 0 | - | - | - | - | - | - | 0.00109 | 0.9693 | 0.0021 |
| Aghabashlo Model – UAD | 3 | - | 0.1199 | 0 | - | - | - | - | - | - | $3.901 \times 10^{-5}$ | 0.9413 | 0.0041 |
| | 6 | - | 0.1125 | 0 | - | - | - | - | - | - | 0.00078 | 0.9944 | 0.0182 |
| | 9 | - | 0.0745 | 0 | - | - | - | - | - | - | | 0.9671 | 0.0894 |
| Aghabashlo Model – MVD | 3 | - | 0.2350 | 0.0109 | - | - | - | - | - | - | $8.33 \times 10^{-6}$ | 0.9980 | 0.0019 |
| | 6 | - | 0.1834 | 0 | - | - | - | - | - | - | 0.00025 | 0.9743 | 0.0103 |
| | 9 | - | 0.1172 | 0 | - | - | - | - | - | - | $8.479 \times 10^{-5}$ | 0.9684 | 0.0060 |
| Hii et al.- OVD | 3 | 0.4071 | - | - | 1.3348 | 0.4867 | - | 0.4867 | 0.4071 | - | $9.8314 \times 10^{-5}$ | 0.9814 | 0.0065 |
| | 6 | 0.2871 | - | - | 1.2049 | 0.4881 | - | 0.4881 | 0.4881 | - | $9.3115 \times 10^{-5}$ | 0.9885 | 0.0063 |
| | 9 | 0.0601 | - | - | 1.6028 | 0.4162 | - | 0.5556 | 0.0601 | - | $4.6905 \times 10^{-5}$ | 0.9962 | 0.0045 |
| Hii et al. – UAD | 3 | 0.0257 | - | - | 1.6959 | 0.4546 | - | 0.4546 | 0.0257 | - | 0.00028 | 0.9665 | 0.0110 |
| | 6 | 0.0894 | - | - | 1.1249 | 0.5019 | - | 0.5019 | 0.0894 | - | $4.754 \times 10^{-6}$ | 0.9957 | 0.0014 |
| | 9 | 0.0167 | - | - | 1.5807 | 0.4639 | - | 0.4639 | 0.0167 | - | 0.00051 | 0.9852 | 0.0148 |
| Hii et al. – MVD | 3 | 0.2664 | - | - | 1.4288 | 0.4942 | - | 0.4942 | 0.2664 | - | $4.243 \times 10^{-5}$ | 0.9913 | 0.0043 |
| | 6 | 0.0818 | - | - | 1.4658 | 0.4852 | - | 0.4852 | 0.0818 | - | $9.887 \times 10^{-5}$ | 0.9916 | 0.0065 |
| | 9 | 0.0395 | - | - | 1.4841 | 0.4733 | - | 0.4733 | 0.0395 | - | 0.00039 | 0.9842 | 0.0004 |
| Lewis - OVD | 3 | 0.5152 | - | - | - | - | - | - | - | - | $6.1147 \times 10^{-7}$ | 0.9705 | 0.00072 |
| | 6 | 0.3229 | - | - | - | - | - | - | - | - | 0.01094 | 0.9882 | 0.09924 |
| | 9 | 0.1604 | - | - | - | - | - | - | - | - | 0.00057 | 0.9656 | 0.02245 |
| Lewis - UAD | 3 | 0.1199 | - | - | - | - | - | - | - | - | $1.0641 \times 10^{-5}$ | 0.9413 | 0.00312 |
| | 6 | 0.1151 | - | - | - | - | - | - | - | - | 0.00017 | 0.9972 | 0.01286 |
| | 9 | 0.0777 | - | - | - | - | - | - | - | - | $3.1926 \times 10^{-5}$ | 0.9643 | 0.00551 |
| Lewis - MVD | 3 | 0.3970 | - | - | - | - | - | - | - | - | $3.1606 \times 10^{-6}$ | 0.9730 | 0.00154 |
| | 6 | 0.1833 | - | - | - | - | - | - | - | - | $9.3369 \times 10^{-6}$ | 0.9743 | 0.00911 |
| | 9 | 0.1172 | - | - | - | - | - | - | - | - | $1.9517 \times 10^{-5}$ | 0.9684 | 0.00425 |
| Two term - OVD | 3 | 0.0173 | 0.5306 | - | - | 0 | 1.0248 | - | - | - | 0.00042 | 0.9687 | 0.0134 |
| | 6 | 0.0338 | 0.3682 | - | - | 0 | 1.0177 | - | - | - | 0.00039 | 0.9831 | 0.0130 |
| | 9 | 0.0177 | 0.1862 | - | - | 0 | 1.0718 | - | - | - | 0.00149 | 0.9632 | 0.0253 |
| Two term - UAD | 3 | 0 | 0.1239 | - | - | 0 | 1.0254 | - | - | - | 0.00142 | 0.9288 | 0.0247 |
| | 6 | 0 | 0.1202 | - | - | 0 | 1.0351 | - | - | - | 0.00018 | 0.9931 | 0.0089 |
| | 9 | 0 | 0.0822 | - | - | 0 | 1.0453 | - | - | - | 0.0041 | 0.9603 | 0.0417 |
| Two term - MVD | 3 | 0.0273 | 0.4111 | - | - | 0 | 1.0318 | - | - | - | 0.00039 | 0.9707 | 0.0129 |
| | 6 | 0 | 0.1951 | - | - | 0 | 1.0546 | - | - | - | 0.00130 | 0.9701 | 0.0236 |
| | 9 | 0 | 0.1238 | - | - | 0 | 1.0468 | - | - | - | 0.00238 | 0.9646 | 0.0327 |
| Diffusion Approximation - OVD | 3 | 0.5152 | - | - | - | 1 | 1 | - | - | - | $1.2294 \times 10^{-6}$ | 0.9705 | 0.0007 |
| | 6 | 0.3603 | - | - | - | 1 | 1 | - | - | - | $1.3159 \times 10^{-5}$ | 0.9841 | 0.0024 |
| | 9 | 0.1714 | - | - | - | 1 | 1 | - | - | - | 0.00109 | 0.9693 | 0.0217 |

(*continued on next page*)

**Table 4** (*continued*)

| Model name | Thickness (mm) | Model parameters | | | | | | | | | $\chi^2$ | $R^2$ | RMSE |
|---|---|---|---|---|---|---|---|---|---|---|---|---|---|
| | | k or $k_0$ | $k_1$ | $k_2$ | n | a | b | c | g | h | | | |
| Diffusion Approximation - UAD | 3 | 0.1199 | - | - | - | 1 | 1 | - | - | - | $3.9018 \times 10^{-5}$ | 0.9413 | 0.0041 |
| | 6 | 1 | - | - | - | 1 | 0.1151 | - | - | - | 0.00077 | 0.994 | 0.0018 |
| | 9 | 0.7512 | - | - | - | 0 | 0.1035 | - | - | - | 0.00020 | 0.9643 | 0.0093 |
| Diffusion Approximation - MVD | 3 | 0.3972 | - | - | - | 1 | 1 | - | - | - | $3.161 \times 10^{-6}$ | 0.9730 | 0.0012 |
| | 6 | 0.1834 | - | - | - | 1 | 1 | - | - | - | 0.00025 | 0.9743 | 0.0103 |
| | 9 | 0.1172 | - | - | - | 1 | 1 | - | - | - | $8.458 \times 10^{-5}$ | 0.9684 | 0.0060 |
| Modified Henderson and Pabis - OVD | 3 | 0.5306 | - | - | - | 0.3416 | 0.3416 | 0.3416 | 0.5306 | 0.5306 | 0.00042 | 0.9687 | 0.0134 |
| | 6 | 0.3682 | - | - | - | 0.3393 | 0.3393 | 0.3393 | 0.3682 | 0.3682 | 0.00039 | 0.9831 | 0.0130 |
| | 9 | 0.1862 | - | - | - | 0.3572 | 0.3572 | 0.3572 | 0.1862 | 0.1862 | 0.00150 | 0.9632 | 0.0253 |
| Modified Henderson and Pabis - UAD | 3 | 0.1239 | - | - | - | 0.3148 | 0.3418 | 0.3418 | 0.1239 | 0.1239 | 0.00142 | 0.9388 | 0.0247 |
| | 6 | 0.1202 | - | - | - | 0.2450 | 0.3450 | 0.3450 | 0.1202 | 0.1202 | 0.00018 | 0.9938 | 0.0089 |
| | 9 | 0.0822 | - | - | - | 0.3484 | 0.3484 | 0.3484 | 0.0822 | 0.0822 | 0.00401 | 0.9602 | 0.0417 |
| Modified Henderson and Pabis - MVD | 3 | 0.4111 | - | - | - | 0.3439 | 0.3439 | 0.3439 | 0.4111 | 0.4111 | 0.00039 | 0.9702 | 0.0129 |
| | 6 | 0.1951 | - | - | - | 0.3515 | 0.3515 | 0.3515 | 0.1951 | 0.1951 | 0.00130 | 0.9701 | 0.0236 |
| | 9 | 0.1196 | - | - | - | 0.8792 | 0.0704 | 0.0878 | 0.1196 | 0.1196 | 0.00108 | 0.9738 | 0.0215 |
| Page - OVD | 3 | 0.4406 | | | 1.2637 | - | - | - | - | - | 0.00038 | 0.9803 | 0.01653 |
| | 6 | 0.2211 | | | 1.3778 | - | - | - | - | - | 0.02142 | 0.9856 | 0.13090 |
| | 9 | 0.0733 | | | 1.5085 | - | - | - | - | - | 0.00037 | 0.9954 | 0.01716 |
| Page- UAD | 3 | 0.0648 | | | 1.3099 | - | - | - | - | - | 0.00197 | 0.9577 | 0.04050 |
| | 6 | 0.0875 | | | 1.1330 | - | - | - | - | - | 0.00049 | 0.9957 | 0.00049 |
| | 9 | 0.0348 | | | 1.3273 | - | - | - | - | - | 0.00177 | 0.9800 | 0.03998 |
| Page - MVD | 3 | 0.2773 | | | 1.4005 | - | - | - | - | - | 0.00026 | 0.9910 | 0.01145 |
| | 6 | 0.0983 | | | 1.3790 | - | - | - | - | - | 0.00042 | 0.9907 | 0.01816 |
| | 9 | 0.0607 | | | 1.3162 | - | - | - | - | - | 0.00105 | 0.9815 | 0.03006 |
| Verma et al.- OVD | 3 | 0.9106 | - | - | - | 15.7084 | - | - | 0.9514 | - | 0.00049 | 0.9809 | 0.0145 |
| | 6 | 0.5784 | - | - | - | 16.9990 | - | - | 0.5973 | - | 0.00051 | 0.9890 | 0.0148 |
| | 9 | 0.3561 | - | - | - | 15.9334 | - | - | 0.3779 | - | 0.00081 | 0.9927 | 0.0186 |
| Verma et al. - UAD | 3 | 0.2198 | - | - | - | 16.8925 | - | - | 0.2293 | - | 0.00432 | 0.9575 | 0.0430 |
| | 6 | 0.1827 | - | - | - | 15.8819 | - | - | 0.1889 | - | $2.759 \times 10^{-5}$ | 0.9956 | 0.0034 |
| | 9 | 0.1443 | - | - | - | 13.6309 | - | - | 0.1526 | - | 0.00721 | 0.9794 | 0.0556 |
| Verma et al. - MVD | 3 | 0.7634 | - | - | - | 14.0130 | - | - | 0.8112 | - | 0.00015 | 0.9698 | 0.0081 |
| | 6 | 0.3449 | - | - | - | 9.07350 | - | - | 0.3788 | - | 0.00077 | 0.9897 | 0.0181 |
| | 9 | 0.2154 | - | - | - | 16.8969 | - | - | 0.2252 | - | 0.00295 | 0.9814 | 0.0356 |
| Henderson and Pabis - OVD | 3 | 0.5306 | - | - | - | 1.0248 | - | - | - | - | 0.00025 | 0.9687 | 0.01343 |
| | 6 | 0.3418 | - | - | - | 1.0461 | - | - | - | - | 0.01947 | 0.9862 | 0.12483 |
| | 9 | 0.1749 | - | - | - | 1.0720 | - | - | - | - | 0.00054 | 0.9591 | 0.02040 |
| Henderson and Pabis - UAD | 3 | 0.1239 | - | - | - | 1.0254 | - | - | - | - | 0.00042 | 0.9388 | 0.01880 |
| | 6 | 0.1202 | - | - | - | 1.0351 | - | - | - | - | $4.5775 \times 10^{-5}$ | 0.9931 | 0.00626 |
| | 9 | 0.0821 | - | - | - | 1.0453 | - | - | - | - | 0.00068 | 0.9603 | 0.02468 |
| Henderson and Pabis - MVD | 3 | 0.4111 | - | - | - | 1.0317 | - | - | - | - | 0.00058 | 0.9707 | 0.01705 |
| | 6 | 0.1951 | - | - | - | 1.0545 | - | - | - | - | 0.00056 | 0.9701 | 0.02082 |
| | 9 | 0.1238 | - | - | - | 1.0468 | - | - | - | - | 0.00062 | 0.9646 | 0.02311 |

ln (MR) against the drying time. The slope of the graph (K) was used in Eq. (7) to calculate the effective moisture diffusivity.

$$MR = \frac{M_{cx} - M_e}{M_i - M_e} = \frac{8}{\pi^2} \exp\left(\frac{-\pi^2 D_{eff} t}{4L^2}\right) \tag{6}$$

$$K = \frac{\pi^2 D_{eff} t}{4L^2}, \qquad D_{eff} = \frac{4KL^2}{\pi^2 t} \tag{7}$$

### 2.5. Colour changes

The Hunterlab Colourflex ® EZ colorimeter (Hunter Associates laboratory, Inc., USA) was used to determine the surface colour of fresh and dried mango slices. Prior to performing measurements calibration was done using black and white standardisation tiles. Mango slices were placed at a random on the colorimeter's cover glass and covered with a cup to prevent light from escaping from the instrument during measurements of the mean Hunter $L^*$, $a^*$ and $b^*$ coordinates. The $L^*$ value represents the sample's lightness which ranges from black (zero) to white (100), the $a^*$ values represents the red (+) and green (-) colours and $b^*$ value represents the yellow (+) and blue (-) colours. The hue angle, chroma and total colour change (ΔE) were calculated from the $L^*$, $a^*$ and $b^*$ colour values using Eqs. (8), (9), and (10), respectively (Akoy, 2014a).

$$Hue\ angle = tan^{-1}\left(\frac{b}{a}\right) \tag{8}$$

$$Chroma = \sqrt{a^2 + b^2} \tag{9}$$

**Table 5.** Goodness of fit parameters obtained by fitting selected moisture ratio models on the experimental data for samples treated with lemon juice.

| Model name | Thickness (mm) | Model parameters | | | | | | | | | $\chi^2$ | $R^2$ | RMSE |
|---|---|---|---|---|---|---|---|---|---|---|---|---|---|
| | | k or $k_0$ ($hr^{-1}$) | $k_1$ | $k_2$ | n | a | b | c | g | h | | | |
| Demil et al.- OVD | 3 | 0.3369 | - | - | 1.4609 | 0.9722 | 0 | - | - | - | $6.8392 \times 10^{-5}$ | 0.9832 | 0.0054 |
| | 6 | 0.1644 | - | - | 1.5382 | 0.9584 | 0 | - | - | - | 0.00010 | 0.9836 | 0.0066 |
| | 9 | 0.0511 | - | - | 1.6609 | 0.9708 | 0 | - | - | - | $5.1271 \times 10^{-5}$ | 0.9959 | 0.0047 |
| Demil et al.- UAD | 3 | 0.0257 | - | - | 1.6958 | 0.9093 | 0 | - | - | - | 0.00028 | 0.9665 | 0.0003 |
| | 6 | 0.0559 | - | - | 0.9659 | 1.2904 | 0 | - | - | - | 0.00010 | 0.9914 | 0.0067 |
| | 9 | 0.0168 | - | - | 1.5289 | 0.9354 | 0 | - | - | - | 0.00029 | 0.9818 | 0.0113 |
| Demil et al. -MVD | 3 | 0.2475 | - | - | 1.4978 | 0.9883 | 0 | - | - | - | $4.014 \times 10^{-5}$ | 0.9929 | 0.0042 |
| | 6 | 0.1066 | - | - | 1.3686 | 0.9761 | 0 | - | - | - | $8.819 \times 10^{-5}$ | 0.9948 | 0.0062 |
| | 9 | 0.0478 | - | - | 1.4194 | 0.9536 | 0 | - | - | - | 0.00028 | 0.9903 | 0.0109 |
| Midilli et al.-OVD | 3 | 0.3369 | - | - | 1.4607 | 0.9722 | 0 | - | - | - | $6.8307 \times 10^{-5}$ | 0.9832 | 0.00541 |
| | 6 | 0.1643 | - | - | 1.5382 | 0.9584 | 0 | - | - | - | $5.0239 \times 10^{-5}$ | 0.9836 | 0.00549 |
| | 9 | 0.0512 | - | - | 1.6609 | 0.9708 | 0 | - | - | - | $3.0819 \times 10^{-5}$ | 0.9959 | 0.00414 |
| Midilli et al. -UAD | 3 | 0.0077 | - | - | 2.2222 | 0.9138 | 0 | - | - | - | $7.9418 \times 10^{-5}$ | 0.9662 | 0.00711 |
| | 6 | 0.0559 | - | - | 1.2903 | 0.9659 | 0 | - | - | - | $3.1126 \times 10^{-5}$ | 0.9932 | 0.00472 |
| | 9 | 0.0166 | - | - | 1.5322 | 0.9351 | 0 | - | - | - | $5.9648 \times 10^{-5}$ | 0.9818 | 0.00691 |
| Midilli et al.-MVD | 3 | 0.2475 | - | - | 1.4978 | 0.9883 | 0 | - | - | - | $4.2402 \times 10^{-5}$ | 0.9929 | 0.00548 |
| | 6 | 0.0604 | - | - | 1.6372 | 0.8888 | 0 | - | - | - | $6.7893 \times 10^{-6}$ | 0.9981 | 0.00194 |
| | 9 | 0.0478 | - | - | 1.4193 | 0.9536 | 0 | - | - | - | $8.2897 \times 10^{-5}$ | 0.9903 | 0.00769 |
| Aghabashlo model- OVD | 3 | - | 0.4689 | 0 | - | - | - | - | - | - | 0.00011 | 0.9646 | 0.0069 |
| | 6 | - | 0.3046 | 0 | - | - | - | - | - | - | 0.00049 | 0.9622 | 0.0144 |
| | 9 | - | 0.1634 | 0 | - | - | - | - | - | - | 0.00161 | 0.9647 | 0.0262 |
| Aghabashlo model – UAD | 3 | - | 0.1199 | 0 | - | - | - | - | - | - | $3.901 \times 10^{-5}$ | 0.9414 | 0.0041 |
| | 6 | - | 0.1036 | 0 | - | - | - | - | - | - | 0.00921 | 0.9857 | 0.0062 |
| | 9 | - | 0.0662 | 0 | - | - | - | - | - | - | 0.01963 | 0.9662 | 0.0917 |
| Aghabashlo model – MVD | 3 | - | 0.3934 | 0 | - | - | - | - | - | - | $1.728 \times 10^{-5}$ | 0.9694 | 0.0027 |
| | 6 | - | 0.1989 | 0 | - | - | - | - | - | - | $1.583 \times 10^{-5}$ | 0.9827 | 0.0044 |
| | 9 | - | 0.1212 | 0 | - | - | - | - | - | - | $4.9297 \times 10^{-5}$ | 0.9774 | 0.0043 |
| Hii et al.- OVD | 3 | 0.3369 | - | - | 1.4608 | 0.4861 | - | 0.4861 | 0.3369 | - | $6.8459 \times 10^{-5}$ | 0.9832 | 0.0054 |
| | 6 | 0.1644 | - | - | 1.5382 | 0.4792 | - | 0.4792 | 0.1644 | - | 0.00010 | 0.9836 | 0.0065 |
| | 9 | 0.0512 | - | - | 1.6609 | 0.4252 | - | 0.5457 | 0.0512 | - | $5.1196 \times 10^{-5}$ | 0.9959 | 0.0046 |
| Hii et al. – UAD | 3 | 0.0257 | - | - | 1.6960 | 0.4546 | - | 0.4546 | 0.0257 | - | 0.00028 | 0.9665 | 0.0111 |
| | 6 | 0.0559 | - | - | 1.2904 | 0.4829 | - | 0.4829 | 0.0559 | - | 0.00010 | 0.9914 | 0.0067 |
| | 9 | 0.0168 | - | - | 1.5288 | 0.4678 | - | 0.4678 | 0.0168 | - | 0.00030 | 0.9818 | 0.0113 |
| Hii et al. – MVD | 3 | 0.2475 | - | - | 1.4977 | 0.4942 | - | 0.4942 | 0.2475 | - | $4.012 \times 10^{-5}$ | 0.9929 | 0.0041 |
| | 6 | 0.1066 | - | - | 1.3685 | 0.4881 | - | 0.4881 | 0.1066 | - | $8.812 \times 10^{-5}$ | 0.9948 | 0.0062 |
| | 9 | 0.0478 | - | - | 1.4193 | 0.4768 | - | 0.4768 | 0.0478 | - | 0.00027 | 0.9903 | 0.0108 |
| Lewis - OVD | 3 | 0.4783 | - | - | - | - | - | - | - | - | 0.00052 | 0.9633 | 0.02130 |
| | 6 | 0.2714 | - | - | - | - | - | - | - | - | 0.00859 | 0.9689 | 0.08791 |
| | 9 | 0.1634 | - | - | - | - | - | - | - | - | 0.00061 | 0.9647 | 0.02319 |
| Lewis - UAD | 3 | 0.1045 | - | - | - | - | - | - | - | - | 0.00066 | 0.9089 | 0.02449 |
| | 6 | 0.1081 | - | - | - | - | - | - | - | - | $2.5591 \times 10^{-5}$ | 0.9884 | 0.00487 |
| | 9 | 0.0695 | - | - | - | - | - | - | - | - | 0.00194 | 0.9635 | 0.04297 |
| Lewis - MVD | 3 | 0.3934 | - | - | - | - | - | - | - | - | $1.7272 \times 10^{-5}$ | 0.9694 | 0.00359 |
| | 6 | 0.1989 | - | - | - | - | - | - | - | - | $1.7186 \times 10^{-5}$ | 0.9827 | 0.00391 |
| | 9 | 0.1213 | - | - | - | - | - | - | - | - | $1.0145 \times 10^{-5}$ | 0.9774 | 0.00307 |
| Two term-OVD | 3 | 0.0191 | 0.4914 | - | - | 0 | 1.0381 | - | - | - | 0.00042 | 0.9614 | 0.0135 |
| | 6 | 0.0283 | 0.3236 | - | - | 0 | 1.0473 | - | - | - | 0.00074 | 0.9581 | 0.0178 |
| | 9 | 0.0177 | 0.1788 | - | - | 0 | 1.0764 | - | - | - | 0.00146 | 0.9577 | 0.0250 |
| Two term-UAD | 3 | 0 | 0.1239 | - | - | 0 | 1.0254 | - | - | - | 0.00142 | 0.9388 | 0.0246 |
| | 6 | 0 | 0.1123 | - | - | 0 | 1.0297 | - | - | - | 0.00076 | 0.9821 | 0.1799 |
| | 9 | 0 | 0.0733 | - | - | 0 | 1.0396 | - | - | - | 0.00213 | 0.9602 | 0.0301 |
| Two term -MVD | 3 | 0 | 0.4097 | - | - | 0 | 1.0376 | - | - | - | 0.00047 | 0.9665 | 0.0141 |
| | 6 | 0 | 0.2093 | - | - | 0 | 1.0464 | - | - | - | 0.00121 | 0.9796 | 0.0228 |
| | 9 | 0 | 0.1276 | - | - | 0 | 1.0439 | - | - | - | 0.00220 | 0.9741 | 0.0309 |
| Diffusion Approximation-OVD | 3 | 0.4689 | - | - | - | 1 | 1 | - | - | - | 0.00011 | 0.9646 | 0.0069 |
| | 6 | 0.3046 | - | - | - | 1 | 1 | - | - | - | 0.00049 | 0.9622 | 0.0144 |
| | 9 | 0.1634 | - | - | - | 1 | 1 | - | - | - | 0.00161 | 0.9647 | 0.0263 |

(*continued on next page*)

**Table 5** (*continued*)

| Model name | Thickness (mm) | Model parameters | | | | | | | | | $\chi^2$ | $R^2$ | RMSE |
|---|---|---|---|---|---|---|---|---|---|---|---|---|---|
| | | k or $k_0$ ($hr^{-1}$) | $k_1$ | $k_2$ | n | a | b | c | g | h | | | |
| Diffusion Approximation -UAD | 3 | 0.1199 | - | - | - | 1 | 1 | - | - | - | $3.902 \times 10^{-5}$ | 0.9413 | 0.0041 |
| | 6 | 0.8858 | - | - | - | 0 | 0.1221 | - | - | - | 0.00011 | 0.9839 | 0.0069 |
| | 9 | 0.7102 | - | - | - | 0 | 0.0979 | - | - | - | 0.00676 | 0.9635 | 0.0170 |
| Diffusion Approximation -MVD | 3 | 0.3934 | - | - | - | 1 | 1 | - | - | - | $1.727 \times 10^{-5}$ | 0.9694 | 0.0027 |
| | 6 | 0.1989 | - | - | - | 1 | 1 | - | - | - | $4.583 \times 10^{-5}$ | 0.9827 | 0.0044 |
| | 9 | 0.1213 | - | - | - | 1 | 1 | - | - | - | $4.396 \times 10^{-5}$ | 0.9774 | 0.0043 |
| Modified Henderson and Pabis - OVD | 3 | 0.4914 | - | - | - | 0.3460 | 0.3460 | 0.3460 | 0.4914 | 0.4914 | 0.00042 | 0.9614 | 0.0134 |
| | 6 | 0.3236 | - | - | - | 0.3491 | 0.3491 | 0.3491 | 0.3236 | 0.3236 | 0.00074 | 0.9581 | 0.0177 |
| | 9 | 0.1788 | - | - | - | 0.3588 | 0.3588 | 0.3588 | 0.1788 | 0.1788 | 0.00146 | 0.9577 | 0.0250 |
| Modified Henderson and Pabis - UAD | 3 | 0.1239 | - | - | - | 0.3418 | 0.3419 | 0.3418 | 0.1239 | 0.1239 | 0.00142 | 0.9388 | 0.0246 |
| | 6 | 0.1123 | - | - | - | 0.3432 | 0.3432 | 0.3432 | 0.1123 | 0.1223 | 0.00075 | 0.9821 | 0.0179 |
| | 9 | 0.0733 | - | - | - | 0.3465 | 0.3465 | 0.3465 | 0.0733 | 0.0733 | 0.00213 | 0.9602 | 0.0302 |
| Modified Henderson and Pabis - MVD | 3 | 0.4097 | - | - | - | 0.3459 | 0.3459 | 0.3459 | 0.4097 | 0.4097 | 0.00047 | 0.9665 | 0.0141 |
| | 6 | 0.2093 | - | - | - | 0.3488 | 0.2488 | 0.3488 | 0.2093 | 0.2093 | 0.00120 | 0.9796 | 0.0228 |
| | 9 | 0.1276 | - | - | - | 0.3479 | 0.3479 | 0.3479 | 0.1276 | 0.1276 | 0.00220 | 0.9741 | 0.0309 |
| Page - OVD | 3 | 0.3714 | - | - | | 1.3724 | - | - | - | - | 0.00037 | 0.9821 | 0.01634 |
| | 6 | 0.2048 | - | - | | 1.3889 | - | - | - | - | 0.00059 | 0.9815 | 0.02166 |
| | 9 | 0.0637 | - | - | | 1.5573 | - | - | - | - | 0.00043 | 0.9949 | 0.01822 |
| Page - UAD | 3 | 0.0282 | - | - | | 1.6637 | - | - | - | - | 0.00283 | 0.9550 | 0.04810 |
| | 6 | 0.0072 | - | - | | 1.1963 | - | - | - | - | 0.00033 | 0.9901 | 0.01744 |
| | 9 | 0.0334 | - | - | | 1.2945 | - | - | - | - | 0.00126 | 0.9772 | 0.03370 |
| Page - MVD | 3 | 0.2583 | - | - | | 1.4675 | - | - | - | - | 0.00026 | 0.9927 | 0.01140 |
| | 6 | 0.1213 | - | - | | 1.3078 | - | - | - | - | 0.00029 | 0.9942 | 0.01523 |
| | 9 | 0.0673 | - | - | | 1.2852 | - | - | - | - | 0.00013 | 0.9897 | 0.01078 |
| Verma et al.- OVD | 3 | 0.9048 | - | - | - | 15.7087 | - | - | 0.9525 | - | 0.00042 | 0.9811 | 0.0133 |
| | 6 | 0.6006 | - | - | - | 17.6556 | - | - | 0.6292 | - | 0.00098 | 0.9801 | 0.0204 |
| | 9 | 0.3437 | - | - | - | 10.5627 | - | - | 0.3779 | - | 0.00091 | 0.9914 | 0.0198 |
| Verma et al. - UAD | 3 | 0.2198 | - | - | - | 16.893 | - | - | 0.2293 | - | 0.00432 | 0.9575 | 0.0430 |
| | 6 | 0.1850 | - | - | - | 16.056 | - | - | 0.1924 | - | 0.00099 | 0.9911 | 0.0206 |
| | 9 | 0.1289 | - | - | - | 13.942 | - | - | 0.1359 | - | 0.00483 | 0.9773 | 0.0455 |
| Verma et al. - MVD | 3 | 0.7869 | - | - | - | 14.216 | - | - | 0.8397 | - | 0.00016 | 0.9907 | 0.0083 |
| | 6 | 0.3612 | - | - | - | 13.1806 | - | - | 0.3827 | - | 0.00057 | 0.9940 | 0.0156 |
| | 9 | 0.2186 | - | - | - | 16.8979 | - | - | 0.2281 | - | 0.00227 | 0.9884 | 0.0311 |
| Henderson and Pabis.- OVD | 3 | 0.4914 | - | - | - | 1.0381 | - | | | | 0.00025 | 0.9614 | 0.01348 |
| | 6 | 0.3236 | - | - | - | 1.0473 | - | | | | 0.00028 | 0.9581 | 0.01486 |
| | 9 | 0.1788 | - | - | - | 1.0763 | - | | | | 0.00063 | 0.9577 | 0.02208 |
| Henderson and Pabis - UAD | 3 | 0.1139 | - | - | - | 1.0609 | - | | | | 0.00037 | 0.9017 | 0.01761 |
| | 6 | 0.1123 | - | - | - | 1.0297 | - | | | | 0.00019 | 0.9824 | 0.01272 |
| | 9 | 0.0732 | - | - | - | 1.0396 | - | | | | 0.00035 | 0.9602 | 0.01785 |
| Henderson and Pabis - MVD | 3 | 0.4096 | - | - | - | 1.0376 | - | | | | 0.00069 | 0.9665 | 0.01867 |
| | 6 | 0.2093 | - | - | - | 1.0463 | - | | | | 0.00052 | 0.9796 | 0.02107 |
| | 9 | 0.1276 | - | - | - | 1.0439 | - | | | | 0.00056 | 0.9741 | 0.02188 |

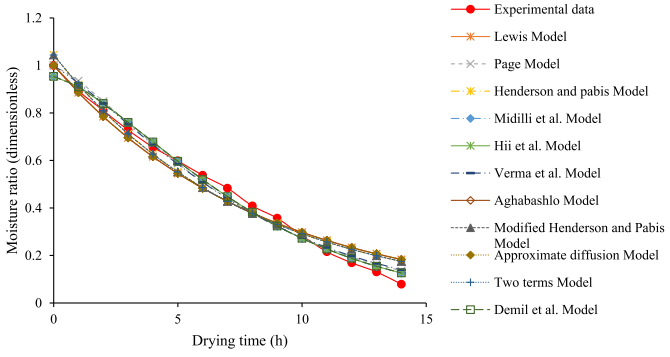


**Figure 4.** The correlation of experimental and predicted moisture ratio for 9 mm lemon juice treated mango samples (MVD).

$$\Delta E = \sqrt{\left(L^*_{dried} - L^*_{fresh}\right)^2 + \left(a^*_{dried} - a^*_{fresh}\right)^2 + \left(b^*_{dried} - b^*_{fresh}\right)^2} \quad (10)$$

### 2.6. Fruit texture

A penetrometer, Instron ® 3345 universal testing machine (Instron, UK), with a 5kN loading capacity was used to measure the texture of fresh mangoes. A 4 mm stainless steel probe was attached to a load cell and penetrated into the fresh mango at a rate of 0.2 $mm.s^{-1}$ and to a depth of 10 mm.

### 2.7. Total soluble solids

A portable refractometer (Atago, PAL-3, Japan) was used to determine the soluble solids concentration (TSS). Distilled water was used to

**Table 6.** $D_{eff}$ values and the coefficient of determination ($R^2$) of the selected drying treatments.

| Drying process | Slice thickness (mm) | $D_{eff}$ ($m^2$. $S^{-1}$) | $R^2$ (dimensionless) |
|---|---|---|---|
| Treated | | | |
| OVD | 3 | $9.7547 \times 10^{-9}$ | 0.895 |
| | 6 | $6.4727 \times 10^{-9}$ | 0.884 |
| | 9 | $3.55545 \times 10^{-9}$ | 0.931 |
| UAD | 3 | $2.46147 \times 10^{-9}$ | 0.783 |
| | 6 | $2.00564 \times 10^{-9}$ | 0.952 |
| | 9 | $1.36748 \times 10^{-9}$ | 0.937 |
| MVD | 3 | $8.29605 \times 10^{-9}$ | 0.932 |
| | 6 | $4.04774 \times 10^{-9}$ | 0.962 |
| | 9 | $2.46748 \times 10^{-9}$ | 0.899 |
| Control | | | |
| OVD | 3 | $1.0484 \times 10^{-8}$ | 0.909 |
| | 6 | $6.74622 \times 10^{-9}$ | 0.939 |
| | 9 | $3.55500 \times 10^{-9}$ | 0.931 |
| UAD | 3 | $2.55263 \times 10^{-9}$ | 0.881 |
| | 6 | $2.00564 \times 10^{-9}$ | 0.945 |
| | 9 | $1.64100 \times 10^{-9}$ | 0.920 |
| MVD | 3 | $8.20489 \times 10^{-9}$ | 0.936 |
| | 6 | $3.82895 \times 10^{-9}$ | 0.949 |
| | 9 | $2.46100 \times 10^{-9}$ | 0.896 |

calibrate the refractometer, at room temperature. TSS values were determined by homogenising a 10 g of fresh mango. The pulp was positioned in the refractometer, and triplicate measurements of TSS were recorded.

### 2.8. Microstructure changes

Mango of both fresh and dried samples, were cut into square-shaped 10 mm × 10 mm pieces. After mounting the pieces on double-sided aluminium stubs, they were coated with a thin layer of gold using a Quorum, Q150RES sputter gold coater (Quorum, UK). The samples were analysed with a Zeiss Evo LS15 scanning electron microscope (SEM) (Zeiss, Germany). The micrographs were taken at a magnification of 300 in a high vacuum with a 5kV accelerating voltage.

### 2.9. Rehydration

The physical and chemical changes that occurred during drying were indicated with rehydration properties. A 250 ml beaker, containing 150 ml of boiled distilled water was used to soak 5 g of the dried mango. The sample was allowed to rehydrate for five minutes. A filter paper was used to separate the water with the rehydrated mango, and the rehydrated mass was determined in triplicate. Utilising Eq. (11), the rehydration ratio was calculated.

$$Rehydration\ ratio = \frac{W_2}{W_1} \tag{11}$$

where the weight $W_2$ (g) and $W_1$ (g) is for the drained and dried mango samples, respectively.

### 2.10. Statistical analysis

The study findings were analysed using one-way Analysis of Variance (ANOVA) and a general Analysis of variance was used to examine the differences between the parameters in VSNI-Genstat (version 18.20.18409). Duncan's multiple comparisons distinguished the mean values at a 95% confidence level.

## 3. Results and discussion

### 3.1. The effect of pre-drying treatments, drying methods and slice thickness on the moisture loss and drying rates

The drying curves exhibited a general trend toward decreasing moisture ratio with increasing drying time until a moisture content of 10 ± 0.9%, as illustrated in Figure 2. Depending on the drying process and slice thickness, the drying time needed to achieve a moisture content of 10 ± 0.9% ranged between 3 and 20 h. The drying rate curves in Figure 3 demonstrated numerous fluctuations in the drying rate, with the most pronounced fluctuations occurring for samples dried in UAD. According to El khadraoui et al. (2019), the drying rate is predicted to fluctuate throughout the hot-air drying process. Additionally, as the drying time increased, the drying rate graphs demonstrated a decreasing drying rate with increasing slice thickness. Drying rates were found to be higher and faster for 3 mm slices than those of 6 mm and 9 mm. When mango slices were dried, Kabiru et al. (2013) observed a similar phenomenon: the maximum drying rate was reached at 3 mm slice thickness, and increasing the thickness to 9 mm resulted in a decreased rate of drying and an increase in drying time. The initial drying time, which was mainly the first hour, had the highest drying rate. Workneh and Oke (2012) established that the rate of drying is relatively higher in the early stages of the drying process, concluding that it is due to increased product's internal temperature (Sadin et al., 2013). The subsequent decrease in drying rate is due to shrinkage of the mango slices, which increased the resistance to water movement, resulting in an additional decrease in drying rate.

Lemon juice pre-drying treatment had no distinct effect on the drying rate ($p > 0.05$). This finding contradicts previous research indicating that pre-drying treatments increase the drying rate by increasing the product porosity, thus facilitating mass transfer (Doymaz, 2004; Sagar and Kumar, 2010; Dinrifo, 2012). As presented in Figure 3 (a-c), the drying rate varied considerably according to the drying method and slice thickness used. For 3 mm samples dried using OVD, this resulted in the highest drying rate of 0.330 $g.h^{-1}$, and the slowest rate was for samples dried in UAD (0.069–0.012 $g.h^{-1}$). Increased drying air temperature accelerates and shortens the drying process (Goyal et al., 2008), due to the increased evaporative air capacity at high air temperatures, water migration and evaporation from the food surface are relatively fast

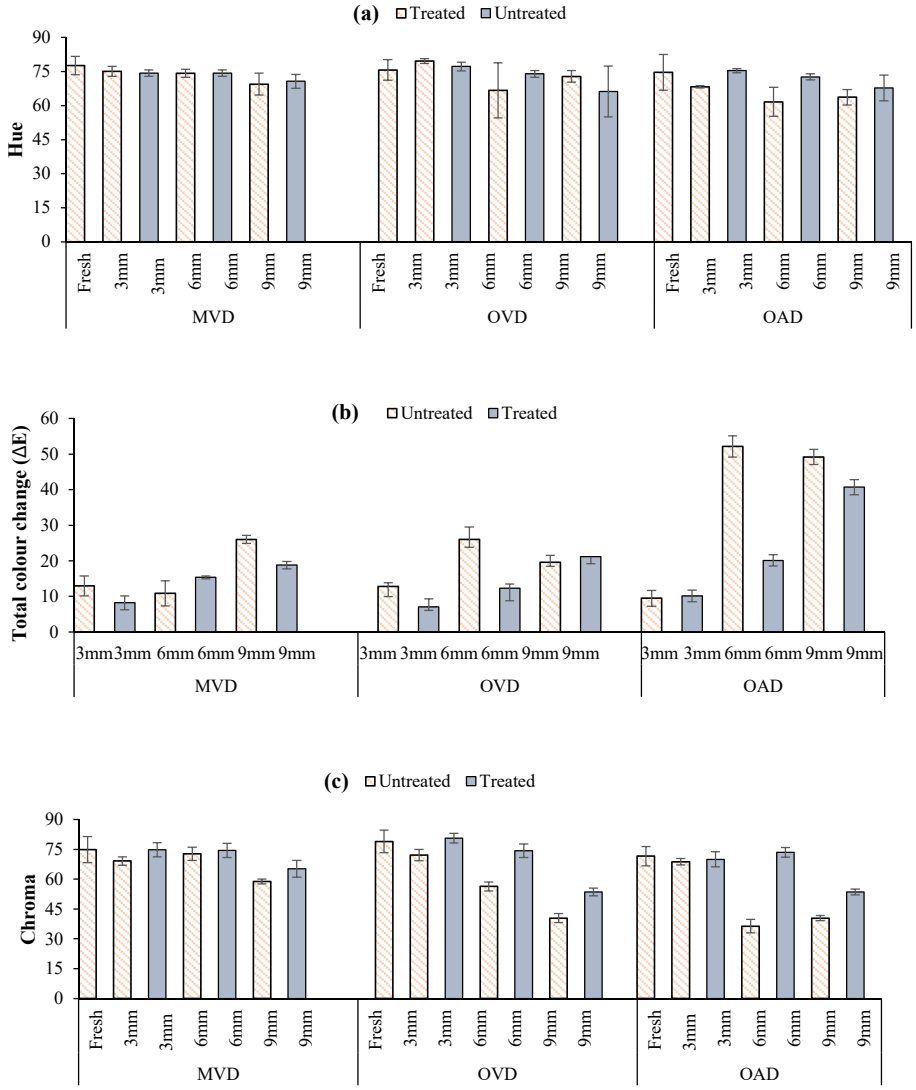


**Figure 5.** Graphical representation of the colour indicators (a) hue angle, (b) total colour change and (c) chroma.

(Fadhel et al., 2014; Vyas and Gojiya, 2014; El khadraoui et al., 2019). Thus, as indicated in Table 1, the MVD's lower relative humidity and increased temperature may have caused faster drying rates and moisture decrease than UAD. Numerous research studies have established that the drying conditions characterised by low relative humidity and high temperatures, such as OVD and MVD, enhance the moisture removal capability of hot-air drying methods (Akoy, 2014b; Fadhel et al., 2014; Murthy and Manohar, 2014). Additionally, other studies have discovered that uncontrolled sun drying of pepper and chilli results in a lower rate of water evaporation than solar drying (Kaewkiew et al., 2012; El khadraoui et al., 2019). Drying of mango samples in OVD and MVD occurred primarily at the falling rate period, whereas for UAD the drying rate was fluctuating throughout the drying process. As a result, the drying process was mainly diffusion-controlled, with moisture being removed from the interior of the mango slices while the surface was continuously drained of water (Rasouli et al., 2011; Doymaz et al., 2015; Onwude et al., 2016). The drying time for the 9 mm samples dried in UAD was approximately twice that of the 3 mm. MVD and OVD shortened the drying time of 3 mm slices by 80% and 85%, respectively (Table 3). Increasing the sample thickness to 6 mm reduced the drying time up to 55 % and 75 %, respectively.

### 3.2. Thin-layer modelling of drying curves

Eleven drying models were statistically analysed using the moisture ratio data, and four models demonstrated a superior fit, namely the Midilli et al., Hii et al., Demil et al. and Aghabashlo models, as shown in Tables 4 and 5. The coefficient of determination ($R^2$), Chi-square ($\chi^2$) and root mean square error (RMSE) were used to predict the model's goodness of fit to the moisture ratio data. Overall, the predictions of the Midilli et al. had the best goodness of fit values, with higher $R^2$, low RMSE and $\chi^2$. The $R^2$ values of the Midilli et al. model varied between 0.9949 and 0.9554 (OVD), 0.9981 and 0.9662 (UAD) and between 0.9981 and 0.9842 for MVD. The RMSE values varied between 0.002 and 0.114 (OVD), 0.001 and 0.009 (UAD) and 0.002 and 0.009 (MVD). The values of $\chi^2$ ranged between $3.082 \times 10^{-4}$ and 0.022 (OVD), $1.45 \times 10^{-6}$ and $5.9 \times 10^{-5}$ (UAD) and $8.29 \times 10^{-5}$ and 0.0001 (MVD). Thus, the Midilli et al. model makes the most accurate predictions of the moisture ratio data for mango slices under the OVD, MVD and UAD drying conditions (Table 1). Other studies have also revealed that the Midilli et al. can best predict the behaviour of mango during hot-air drying (Kabiru et al., 2013; Murthy and Manohar, 2014; Izli et al., 2017).

**Table 7.** Results of the dried mango rehydration ratio.

| Drying process | Treatment | Thickness(mm) | Rehydration ratio (dimensionless) |
|---|---|---|---|
| OVD | Lemon juice treatment | 3 | $2.518 \pm 0.43^{e^{ghi}}$ |
| | | 6 | $1.986 \pm 0.13^{bcdefg}$ |
| | | 9 | $1.152 \pm 0.28^{a}$ |
| | Control | 3 | $2.297 \pm 0.25^{fghi}$ |
| | | 6 | $2.107 \pm 0.17^{cdefgh}$ |
| | | 9 | $1.479 \pm 0.25^{ab}$ |
| MVD | Lemon juice treatment | 3 | $1.919 \pm 0.18^{bcdef}$ |
| | | 6 | $2.352 \pm 0.06^{fghi}$ |
| | | 9 | $1.591 \pm 0.09^{abc}$ |
| | Control | 3 | $2.100 \pm 0.05^{cdefgh}$ |
| | | 6 | $2.542 \pm 0.29^{hi}$ |
| | | 9 | $1.718 \pm 0.26^{bcd}$ |
| OUAD | Lemon juice treatment | 3 | $2.518 \pm 0.18^{ghi}$ |
| | | 6 | $1.649 \pm 0.06^{abcd}$ |
| | | 9 | $1.756 \pm 0.09^{bcde}$ |
| | Control | 3 | $2.667 \pm 0.05^{i}$ |
| | | 6 | $2.171 \pm 0.29^{defghi}$ |
| | | 9 | $1.861 \pm 0.26^{bcdef}$ |

*In a column, mean values (±SD) of identical superscript letters are not statistically different ($p < 0.05$).

### 3.2.1. Comparison of existing thin-layer drying models in predicting the moisture ratio

The general pattern of the experimental and predicted moisture ratio and time was depicted in Figure 4. Overall, the Midilli et al. model had the highest correlation to experimental moisture ratio data for all the drying treatments. Abano et al. (2013) and (Murthy and Manohar, 2014) both observed comparable results in hot air drying and concluded that the Midilli et al. model was the most effective at optimising the co-efficients and predicting the experimental moisture ratio data. The Henderson and Pabis, modified Henderson and Pabis and Two-terms models all overestimate the initial moisture ratio and at the end of the drying process. Whereas Approximate diffusion, Aghabashlo and Lewis models overestimate the final moisture ratio. Demil et al. and Hii et al. models underestimate the initial moisture ratio. As a result, these models were identified to have the lowest correlation with the experimental data. Workneh and Oke (2012) also observed that some models do over- or under- estimate the experimental moisture ratio data during tomato drying.

### 3.3. Effective moisture diffusivity

The effective moisture diffusivity is dependent on both temperature and moisture content and can be used to characterise the complex moisture migration process (Ong and Law, 2020). It was determined by

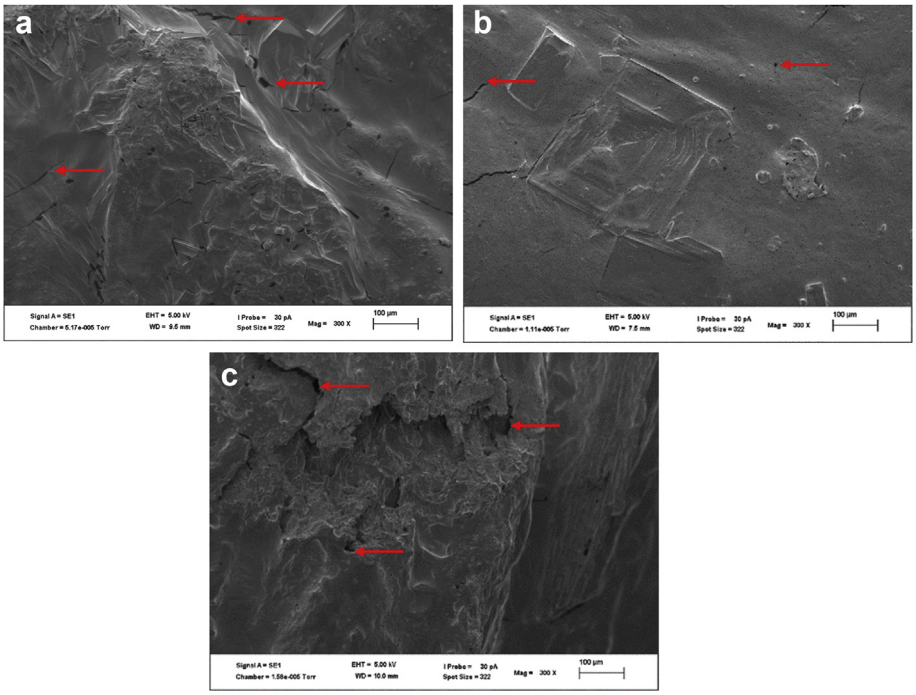


**Figure 6.** Micrographs for 3mm mango samples dried in (a) MVD, (b) OVD and (c) UAD (300 x magnification, 100 μm scale).

the slope of the trendline using the graphical method. The coefficient of determination ($R^2$) of the plotted data was between 78.2% and 94.5% (Table 6), indicating that the Fick's model was applicable in illustrating the $D_{eff}$'s variability. Additionally, Table 6 contains the values of the effective moisture diffusivity which varied between and $9.7547 \times 10^{-9}$ and $1.0484 \times 10^{-8}$ $m^2$. $s^{-1}$. The variation was caused by the mango sample thickness, with 3 mm slicess having a higher $D_{eff}$ than the 6- and 9-mm thickness. Furthermore, OVD exhibited a higher $D_{eff}$ than UAD or MVD. According to (Akoy, 2014b), increasing the air temperature also increase water activity within the product, resulting in increased moisture diffusivity. However, no substantial difference ($p > 0.05$) in $D_{eff}$ was observed between the treated and control samples. This was inconsistent with Dinrifo (2012) findings that treated samples had a greater moisture diffusivity. In general, the $D_{eff}$ of over 80% of the fruits is between $10^{-11}$ and $10^{-8}$ (Onwude et al., 2016). Perumal (2007) reached a similar conclusion to this research, claiming that unregulated solar drying has a lower effective diffusivity than other hot-air drying methods and that thicker materials are inefficient at distributing moisture.

## 4. Quality changes

### 4.1. Colour

The results of the fresh and dried mango sample's surface colour coordinates lightness ($L^*$), redness ($a^*$) and yellowness ($b^*$) were presented on (Mugodo et al., 2020). The interaction between the process of drying, sample thickness and pre-drying treatment had a significant influence on the surface colour coordinates ($p < 0.001$). In general, the increase in the lightness of mango samples dried in OVD and MVD was greater than that of samples dried in UAD. Simultaneously, the redness of the samples increased, except for those dried in OVD. The hue angle values (Figure 5a) indicated that all drying methods and treatments used resulted in a substantial ($p < 0.001$) reduction the yellow colour of mango samples. However, the OVD (78.43–70.35) and MVD (74.72–71) preserved yellowness better than samples dried in UAD. According to Oliveira et al. (2015), the duration of drying is a primary factor that affects the preservation of a product's yellowness. A closer examination of the total change in colour (ΔE), which is a composite of L*, $a^*$, and $b^*$ values (Figure 5b), revealed that OVD (8.21–25.99) had a better ability to preserve the surface colour. However, the ΔE values were all greater than three, indicating that the total colour change caused by UAD, OVD and MVD drying processes was quite distinct (Adekunte et al., 2010). The greatest increase in ΔE was observed in samples that were dried by UAD (9.47–52.16). The total colour increase was higher for thicker samples (6 and 9 mm) and control samples. Similar research found that samples dried at a relatively low temperature, such as in UAD, had higher ΔE values than samples dried in a convective dryer (Akoy, 2014a; Nyangena et al., 2019). Nyangena et al. (2019) concluded that lemon juice as a pre-drying treatment does not prevent colour change during drying. However, this study observed the contrary as the lemon juice pre-drying treatment reduced the total colour change, especially for the 6- and 9-mm mango samples that were dried in UAD, which had prolonged drying times. The primary cause of colour change during drying is carotenoid degradation, non-enzymatic (Maillard reaction), enzymatic reaction or prolonged drying times (Akoy, 2014a; Deng et al., 2017). The degree of colour saturation, as indicated by the chroma in Figure 5c, varied between the fresh and dried samples and decreased in the order MVD < OVD < UAD. Relatively higher colour changes were observed in control samples with 6 mm and 9 mm thickness. As a result of these findings, it is clear that drying results in significant changes in colour parameters, with UAD having the greatest effect.

### 4.2. Rehydration capacity

The rehydration properties were summarised in Table 7. Overall, the rehydration ratio of the mango samples were not statistically different ($p > 0.05$) for all drying treatments. For samples dried in OVD, MVD and UAD, the rehydration ratios varied between $2.518 \pm 0.43$ and $1.512 \pm 0.28$, $2.542 \pm 0.29$ and $1.591 \pm 0.09$ and between $2.667 \pm 0.05$ and $1.649 \pm 0.06$, respectively. As a result, UAD dried samples demonstrated higher rehydration values than MVD- and UAD-dried samples. For each drying process, the rehydration ratio was significantly greater ($p < 0.001$) for 3 mm samples than for the 6 and 9 mm. Pre-drying treatment had no important effect on the rehydration of mango samples ($p > 0.05$). This study confirms the findings by Abano et al. (2013) and Deng et al. (2017), who also concluded that pre-drying treatments, such as lemon juice, have little effect on the rehydration characteristics. However, the results contradict those of Akoy (2014a), who discovered that as the duration of the drying process increased, the rehydration ratio decreased. The highest observed rehydration ratio for UAD may be a result of increased stresses inside the mango samples during prolonged drying times. Reduced rehydration ratios for the 6 and 9 mm samples indicate cell wall damage (Perumal, 2007).

### 4.3. Microstructure changes

The surface microstructure of fresh and dried mango was compared using SEM micrographs. The surface of fresh mangoes was smooth and irregular, and for the dried samples no discernible difference was observed between the pre-treated and control. Notable changes in the microstructure were observed based on the drying technique used. The UAD and MVD microstructures revealed a few small pores, whereas the UAD microstructure revealed large pores, longer and wider cracks, as shown in Figure 6. Additionally, Fazaeli et al. (2015) discovered that water evaporation from the samples, during hot-air drying results in the formation of a porous structure. Corrêa et al. (2010) established that a large vapour pressure gradient created by capillary flow and pressure changes exposes the food structure to such changes. Additionally, other studies concluded that the development of cracks is a direct sign of a damaged cell wall, which is caused by prolonged periods, such as those observed in UAD (Vega-Galvez et al., 2012). In conclusion, UAD disrupts the structure of mango slices, which may explain why the rehydration rates reported in section 4.3 are relatively higher.

## 5. Conclusions

The study discovered that the drying techniques used and the thickness of mango slices have a major effect on the drying kinetics, colour, rehydration and microstructure. The drying time for the optimal thickness (3mm) was significantly reduced by OVD and MVD. Eleven mathematical models for moisture ratio were compared to experimental moisture ratio data, and the Midilli et al. had the largest association with the data. Lemon juice pre-drying treatment had no influence on the drying process, including the drying time, rate or moisture diffusivity. It did, however, have a detrimental effect on the quality. Additionally, thinner samples (3mm) and those that were dried using UAD had the highest rehydration ratio values. Micrographs revealed that samples dried in UAD had numerous cracks and pores. The study established that OVD at 70 °C and a thickness of 3 mm significantly improves the drying process and preserves the product's quality. Finally, while the performance of MVD is similar to that of OVD, measures should be taken to increase the drying temperature for a faster drying process and improved quality preservation, especially when using thicker slices (>3 mm).

## Declarations

### Author contribution statement

Khuthadzo Mugodo: Conceived and designed the experiments; Performed the experiments; Analyzed and interpreted the data; Contributed reagents, materials, analysis tools or data; Wrote the paper.

Tilahun S. Workneh: Contributed reagents, materials, analysis tools or data; Wrote the paper.

*Funding statement*

This work was supported by the Agricultural Research Council.

*Data availability statement*

Data will be made available on request.

*Declaration of interests statement*

The authors declare no conflict of interest.

*Additional information*

No additional information is available for this paper.

## Acknowledgements

The authors would like to acknowledge the University of Kwazulu-Natal for providing the resources for the data collection, analysis and interpretation. Also, we acknowledge ZZ2 for providing us with Tommy Atkin mangoes used for this study experiments.

## References

Abano, E., Sam-Amoah, L., Owusu, J., Engmann, F., 2013. Effects of ascorbic acid, salt, lemon juice, and honey on drying kinetics and sensory characteristic of dried mango. Croat. J. Food Sci. Technol. 5 (1), 1–10.

Adekunte, A., Tiwari, B., Cullen, P., Scannell, A., O'donnell, C., 2010. Effect of sonication on colour, ascorbic acid and yeast inactivation in tomato juice. Food Chem. 122 (3), 500–507.

Aghbashlo, M., kianmehr, M.H., Samimi-Akhijahani, H., 2008. Influence of drying conditions on the effective moisture diffusivity, energy of activation and energy consumption during the thin-layer drying of berberis fruit (Berberidaceae). Energy Convers. Manag. 49 (10), 2865–2871.

Akoy, E., 2014a. Effect of drying temperature on some quality attributes of mango slices. Int. J. Innov. Scient. Res. 4 (2), 91–99.

Akoy, E., 2014b. Experimental characterization and modeling of thin-layer drying of mango slices. Int. Food Res. J. 21 (5), 1911–1917.

AOAC, 2005. Official Methods of Analysis. Association of Official Analytical Chemists, Arlington, VA, USA.

Aphane, M., 2015. Comparing Trends in Global and Domestic Mango Commodity Chains [Internet]. Available from: www.hsrc.ac.za 〉 research-data 〉 ktree-doc. (Accessed 13 January 2020).

Basunia, M., Abe, T., 2001. Thin-layer solar drying characteristics of rough rice under natural convection. J. Food Eng. 47 (4), 295–301.

Corrêa, J.L.G., Pereira, L.M., Vieira, G.S., Hubinger, M.D., 2010. Mass transfer kinetics of pulsed vacuum osmotic dehydration of guavas. J. Food Eng. 96 (4), 498–504.

Crank, J., 1975. Methods of solution when the diffusion coefficient is constant. The mathematics of diffusion, 2, pp. 11–27.

DAFF, 2018. A Profile of the South African Mango Market Value Chain. Department of Agriculture, Forestry and Fisheries (DAFF). Pretoria, South Africa.

Demir, V., Gunhan, T., Yagcioglu, A.K., 2007. Mathematical modelling of convection drying of green table olives. Biosyst. Eng. 98 (1), 47–53.

Deng, L.-Z., Yang, X.-H., Mujumdar, A.S., Zhao, J.-H., Wang, D., Zhang, Q., Wang, J., Gao, Z.-J., Xiao, H.-W., 2017. Red pepper (Capsicum annuum L.) drying: effects of different drying methods on drying kinetics, physicochemical properties, antioxidant capacity, and microstructure. Dry. Technol. 36 (8), 893–907.

Deshmukh, A.W., Varma, M.N., Yoo, C.K., Wasewar, K.L., 2014. Investigation of Solar drying of ginger (Zingiber officinale): emprical modelling, drying characteristics, and quality study. Chin. J. Eng. 2014 (ID 305823), 1–7.

Dhanushkodi, S., Wilson, V.H., Sudhakar, K., 2017. Mathematical modeling of drying behavior of cashew in a solar biomass hybrid dryer. Res. Eff. Technol. 3 (4), 359–364.

Diamante, L., Munro, P., 1993. Mathematical modeling of the thin layer solar drying of sweet potato slices. Sol. Energy 51 (4), 271–276.

Dinrifo, R., 2012. Effects of pre-treatments on drying kinetics of sweet potato slices. Agric. Eng. Int.: CIGR J. 14 (3), 136–145.

Doymaz, İ., 2004. Effect of pre-treatments using potassium metabisulphide and alkaline ethyl oleate on the drying kinetics of apricots. Biosyst. Eng. 89 (3), 281–287.

Doymaz, I., Kipcak, A.S., Piskin, S., 2015. Microwave drying of green bean slices: drying kinetics and physical quality. Czech J. Food Sci. 33 (4), 367–376.

El khadraoui, A., Hamdi, I., Kooli, S., Guizani, A., 2019. Drying of red pepper slices in a solar greenhouse dryer and under open sun: experimental and mathematical investigations. Innovat. Food Sci. Emerg. Technol. 52, 262–270 (2019).

ELkhadraoui, A., Kooli, S., Hamdi, I., Farhat, A., 2015. Experimental investigation and economic evaluation of a new mixed-mode solar greenhouse dryer for drying of red pepper and grape. Renew. Energy 77 (March 2019), 1–8.

Fadhel, A., Kooli, S., Farhat, A., Belghith, A., 2014. Experimental study of the drying of hot red pepper in the open air, under greenhouse and in a solar drier. Int. J. Renew. Energy Biofuel 2014, 1–14 (2014).

FAOSTAT, 2019. Food and Agricultural Data. Food and Agricultural Organization of the United Nations [Internet]Available from: http://www.fao.org/faostat/en/#home. (Accessed 22 August 2020).

Fazaeli, M., Tahmasebi, M., Djomeh, Z., 2015. Characterization of texture: application of microscopic technology. In: Méndez-Vilas, A. (Ed.), Current Microscopy Contributions to Advances in Science and Technology. Formatex Research Center, Badajoz, Spain.

Galán Saúco, V., 2010. Worldwide mango production and market: current situation and future prospects. In: IX International Mango Symposium, 992, pp. 37–48.

Goyal, R.K., Mujjeb, O., Bhargava, V.K., 2008. Mathematical modeling of thin layer drying kinetics of apple in tunnel dryer. Int. J. Food Eng. 4 (8), 1–16.

Hayaloglu, A., Karabulut, I., Alpaslan, M., Kelbaliyev, G., 2007. Mathematical modeling of drying characteristics of strained yoghurt in a convective type tray-dryer. J. Food Eng. 78 (1), 109–117.

Hii, C.L., Law, C.L., Cloke, M., 2009. Modeling using a new thin layer drying model and product quality of cocoa. J. Food Eng. 90 (2), 191–198.

Izli, N., Izli, G., Taskin, O., 2017. Influence of different drying techniques on drying parameters of mango. Food Sci. Technol. 37 (4), 604–612.

Kabiru, A.A., Joshua, A.A., Raji, A.O., 2013. Effect of slice thickness and temperature on the drying kinetics of mango (Mangifera indica). Int. J. Res. Rev. Appl. Sci. 15 (1), 41–50.

Kaewkiew, J., Nabnean, S., Janjai, S., 2012. Experimental investigation of the performance of a large-scale greenhouse type solar dryer for drying chilli in Thailand. Procedia Eng. 32 (2012), 433–439.

Kumar, A., Singh, M., Singh, G., 2013. Effect of different pretreatments on the quality of mushrooms during solar drying. J. Food Sci. Technol. 50 (1), 165–170.

Liu, P., Altendorf, S., Bonavita, G., 2020. Major Tropical Fruits Market Review February 2020 Snapshot. FAO [Internet] Available from: http://www.fao.org/economic/est/est-commodities/tropical-fruits/en/. (Accessed 14 June 2020).

Meisami-asl, E., Rafiee, S., 2009. Mathematical modeling of kinetics of thin-layer drying of apple (var.Golab). Agric. Eng. Int.: CIGR J. XI (2009), 1185–1196.

Mercer, D., 2012. A comparison of the kinetics of mango drying in open-air, solar and forced-air dryers. Afr. J. Food Nutr. Sci. 12 (7), 6835–6852.

Midilli, A., Kucuk, H., Yapar, Z., 2002. A new model for single-layer drying. Dry. Technol. 20 (7), 1503–1513.

Misha, S., Mat, S., Ruslan, M.H., Salleh, E., Sopian, K., 2016. Performance of a solar-assisted solid desiccant dryer for oil palm fronds drying. Sol. Energy 132 (2016), 415–429.

Mitra, S.K., 2016. Mango production in the world – present situation and future prospect. Acta Hortic. 1111, 287–296.

Motevalli, A., Minaei, S., Soufi, M.D., Ghobadian, B., Khostaghava, M., 2013. Investigation of thermal utilization efficiency in different drying methods of Pomegranate Arils. Int. J. Agron. Plant Prod. 4 (8), 2046, 2043.

Mugodo, K., 2017. Evaluation of the Effects of Pre-drying Treatments and Drying Methods on the Drying Kinetics and Quality of Tommy Atkin Mango Slices. Bioresouces Engineering, University of KwaZulu-Natal, Pietermaritzburg, South Africa. Unpublished thesis.

Mugodo, K., Workneh, T.S., Sibanda, S., 2020. Investigating the effects of pre-treatment and thin layer drying methods on quality of mango slices. Acta Hortic. (1292), 129–136.

Murthy, T.P., Manohar, B., 2014. Hot air drying characteristics of mango ginger: prediction of drying kinetics by mathematical modeling and artificial neural network. J. Food Sci. Technol. 51 (12), 3712–3721.

Ntuli, V., Chatanga, P., Kwiri, R., Gadaga, H.T., Gere, J., Matsepo, T., Potloane, R.P., 2017. Microbiological quality of selected dried fruits and vegetables in Maseru, Lesotho. Afr. J. Microbiol. Res. 11 (5), 185–193.

Nyangena, I., Owino, W., Ambuko, J., Imathiu, S., 2019. Effect of selected pretreatments prior to drying on physical quality attributes of dried mango chips. J. Food Sci. Technol. 56 (8), 3854–3863.

Oliveira, S., Ramos, I., Brandão, T., Silva, C., 2015. Effect of air-drying temperature on the quality and bioactive characteristics of dried galega kale (Brassica oleraceaL. Var. Acephala). J. Food Process. Preserv. 39 (6), 2485–2496.

Ong, S., Law, C., 2020. Hygrothermal properties of various foods, vegetables and fruits. In: Jangam, S., Law, C., Mujumdar, A. (Eds.), Drying of Foods, Vegetables and Fruits, Singapore.

Onwude, D.I., Hashim, N., Janius, R.B., Nawi, N.M., Abdan, K., 2016. Modeling the thin-layer drying of fruits and vegetables: a review. Compr. Rev. Food Sci. Food Saf. 15 (3), 599–618.

Perumal, R., 2007. Comparative Performance of Solar Cabinet, Vacuum Assisted Solar and Open Sun Drying Methods. Unpublished Thesis, Bioresources Engineering. McGill University, Montreal, Canada.

Rasouli, M., Ghasemzadeh, H.R., Nalbandi, H., 2011. Convective drying of garlic ('Allium sativum'l.): Part I: drying kinetics, mathematical modeling and change in color. Aust. J. Crop. Sci. 5 (13), 1707.

Sadin, R., Chegini, G.-R., Sadin, H., 2013. The effect of temperature and slice thickness on drying kinetics tomato in the infrared dryer. Heat Mass Tran. 50 (4), 501–507.

Sagar, V., Kumar, S., 2010. Recent advances in drying and dehydration of fruits and vegetables: a review. J. Food Sci. Technol. 47 (1), 15–26.

Touré, S., Kibangu-Nkembo, S., 2004. Comparative study of natural solar drying of cassava, banana and mango. Renew. Energy 29 (6), 975–990.

Tshitiza, O., Phaleng, L., Kala, Z., Lubinga, M., Ntombela, S., 2020. South Africa Fruit Flow Report. National Agricultural Marketing Council, Pretoria, South Africa.

Vega-Galvez, A., Ah-Hen, K., Chacana, M., Vergara, J., Martinez-Monzo, J., Garcia-Segovia, P., Lemus-Mondaca, R., Di Scala, K., 2012. Effect of temperature and air

velocity on drying kinetics, antioxidant capacity, total phenolic content, colour, texture and microstructure of apple (var. Granny Smith) slices. Food Chem. 132 (1), 51–59.
Verma, L., Bucklin, R., Endan, J., Wratten, F., 1985. Effects of drying air parameters on rice drying models. Trans. ASAE 28 (1), 296–301.
Vyas, D., Gojiya, D., 2014. Studies on effect of slice thickness and temperature on drying kinetics of kothimbda (Cucumis Callosus) and its storage. J. Food Process. Technol. 6 (1), 1–8.
Wang, Z., Sun, J., Chen, F., Liao, X., Hu, X., 2007. Mathematical modelling on thin layer microwave drying of apple pomace with and without hot air pre-drying. J. Food Eng. 80 (2), 536–544.
Workneh, T., Oke, M., 2012. The influence of the combined microwave power and hot-air ventilation on the drying kinetics and colour quality of tomato slices. Afr. J. Biotechnol. 11 (87), 15353–15364.